Sex Dependent Regional Differences in Dopamine Release Determined by Chronic Fast-Scan Cyclic Voltammetry in Nucleus Accumbens and Dorsal Striatum

Abbreviated Title: Regional and sex differences in dopamine release

Authors:

Ivette L. Gonzalez[1*], Christopher A. Turner[1*], Paras R. Patel[2], Noah B. Leonardo[1,3], Brandon D. Luma[3], Julianna M. Richie[2], Dawen Cai[4], Cynthia A. Chestek[2,5,6,7], Jill B. Becker[1,3]

[1] Department of Psychology, University of Michigan

[2] Department of Biomedical Engineering, University of Michigan

[3] Michigan Neuroscience Institute, University of Michigan

[4] Department of Cell & Developmental Biology, University of Michigan

[5] Robotics Graduate Program, University of Michigan

[6] Neuroscience Graduate Program, University of Michigan

[7] Department of Electrical Engineering and Computer Science, University of Michigan

*Co-first authors

Corresponding author:

Jill B. Becker

jbbecker@med.umich.edu

Michigan Neuroscience Institute

205 Zina Pitcher Place, Ann Arbor, MI 48109

Abstract

Dopamine (DA) signaling in the nucleus accumbens (NAc) and dorsolateral striatum (DLS) is thought to contribute to sex differences in motivated behaviors. Using a chronic 16-channel carbon fiber electrode, electrical stimulation (ES) induced DA release in freely behaving male and female rats was recorded using fast-scan cyclic voltammetry (FSCV). In the NAc of gonad-intact rats, individually or pair housed, DA release was recorded simultaneously in the core (NAcC) and shell (NAcS) following 60Hz ES of the ventral tegmental area DA cell bodies. Electrode placement was determined post-mortem. No differences were found in stimulated DA release when NAcC and NAcS were recorded simultaneously in either males or females. In females, however, there was greater ES DA release in NAcS of pair-housed females than individually housed females. There was no effect of housing on ES NAc DA release in males. In the DLS of castrated (CAST) male and ovariectomized (OVX) females, DA release following ES of the medial forebrain bundle at 60Hz was studied over four weeks. There were no sex differences in ES DA release of gonadectomized rats. However, ES DA release increased over time for both CAST males and OVX females. In both sexes, reuptake decreased with the number of pulses, but females had slower reuptake at lower stimulation parameters. Using this novel 16-channel chronic FSCV electrode we reliably record stimulated DA release over time. Furthermore, we found sex differences in the effects of social housing in the NAcS and we report sensitization of ES-induced DA release in DLS.

Significance Statement

A novel electrode was used to record stimulated dopamine release over weeks in the nucleus accumbens and dorsolateral striatum of male and female rats. We find that pair housing, compared with individual housing, enhanced stimulated dopamine release in the nucleus accumbens shell, in females, but not males. These findings are important as they demonstrate that housing conditions can differentially affect neurotransmitter responsiveness to stimulation in a location and sex-dependent way. There were no sex-related differences in the dorsolateral striatum of gonadectomized rats. Importantly there was sensitization of electrical stimulation-induced dopamine release in dorsolateral striatum over four weeks. This indicates for the first time that sensitization of stimulated dopamine release can be demonstrated *in vivo* in dorsolateral striatum.

Introduction

The role of the ascending dopamine (DA) system in motivation has long been debated. One theory highlights how phasic DA can represent both a learning signal and motivation for reward (Hamid et al., 2016). Another theory focuses on incentive motivation and DA sensitization as the mediator of craving for drugs of abuse, but not the hedonic value of abused drugs (Samaha et al., 2021). The heterogeneous nature of DA release in striatal subregions has also been noted, but understudied (Floresco, 2015; Rossi et al., 2020).

The nucleus accumbens (NAc), or ventral striatum, can be segregated into two histologically and anatomically distinct subregions known as the core (NAcC) and shell (NAcS). The NAc and dorsolateral striatum (DLS) are topographically innervated by neurons from the ventral tegmental area (VTA) and substantia nigra, respectively, and also receive different cortical afferent innervation (Lynd-Balta and Haber, 1994).

Understanding how DA release varies among these terminal subregions is important for our understanding of the role of DA in motivation and behavior. The NAcC and NAcS respond differently during reward devaluation (West and Carelli, 2016). It would be important for our understanding of the role of DA in these brain regions to be able to record DA during learning tasks. Furthermore, during learning to respond for cocaine in rodents, reward value is initially encoded by DA in the NAc, where it is hypothesized to represent goal directed behavior. As learning of cocaine reward progresses, cue-induced DA in the DLS emerges as DA release induced by the cue in the NAc declines (Willuhn et al., 2012).

Sampling techniques to directly measure DA release *in vivo* have struggled with spatial and/or temporal resolution (Wu et al., 2022). Fast-scan cyclic voltammetry (FSCV) is an electrochemical technique that uses an electrode to measure oxidizable molecules, such as DA with high temporal resolution (Garris and Wightman, 1995). FSCV has been used *in vitro* with brain slices as well as *in vivo* in anesthetized or freely-moving animals (Garris et al., 1997). Acutely implanted electrodes are driven into the brain with a microdrive, however, this approach causes a large amount of damage to neural tissue (Puthongkham et al., 2019). Recordings from chronically implanted electrodes have been used to allow for studies with a more longitudinal design (Clark et al., 2010). Chronic implantation introduces different challenges such as reduced sensitivity due to immune response (Clark et al., 2010). While there have been many

advancements in carbon fiber electrode technology for use in freely moving animals, there are still limitations.

In this project, DA release in freely moving animals was chronically and reliably detected from multiple locations within the NAcC and NacS simultaneously, or in the DLS. To investigate the differences in DA release in the NAcC and NAcS, we employed an electrode that can record from multiple areas simultaneously combined with a method to precisely determine electrode location postmortem. A 16-channel high density carbon fiber (HDCF) electrode array was designed and manufactured (Huan et al., 2021). These probes were then tested for durability and found to maintain reliable high yield recordings for at least two months (Welle et al., 2020).

We took into consideration how to optimize the electrode from a bioengineering perspective as well as a functional perspective. With this probe, basal (DA transients) and ES DA release in the NAcC and NAcS and in the DLS in a freely moving animal is reliably recorded for weeks. The location of the probe is determined post-mortem using slice-in-place technology.

We used these probes to investigate ES DA release in the NAcC and NAcS in male and female rats that were housed either individually or in pairs. We also investigated changes in ES DA release in the DLS of gonadectomized animals over a six-week period.

Materials and Methods

Subjects

Male and female Sprague-Dawley rats were obtained from Charles River Breeding Laboratory (Portage, MI). Animals were maintained on a 14:10 light/dark cycle in a temperature-controlled climate of 72 ± 2 °F, in ventilated laboratory cages. Rats had *ad libitum* access to water and phytoestrogen-free rat chow (2017 Teklad Global, 14% protein rodent maintenance diet, Harlan rat chow; Harlan Teklad). All procedures were performed according to protocols approved by the University of Michigan Institutional Animal Care and Use Committee.

For experiments targeting the NAc, animals were approximately 40-45 days old on arrival (15 females, 15 males). Some animals were individually housed and others were housed in pairs (social housing) for at least two weeks before surgery. Rats were about 75 days old on their first day of testing. For experiments on DLS, 6 male and 5 female rats were used and were approximately 70-75 days old on arrival.

Acquisition Hardware and Software

Data was acquired using two PCIe-7841 R series cards (National Instruments). Each card acquired eight independent streams of analog data, totaling 16 channels for the system. One of the analog outputs from the first card was used to generate the common ramp signal (-0.4 to 1.3 to -0.4 V) at a rate of 400 V/s (8.5 ms duration) after which there was a 91.5 ms hold period at -0.4 V. This signal was continuously repeated at a rate of 10Hz. If the rate was increased to 60Hz the hold period was adjusted accordingly by the software, but the ramp signal stayed the same.

The ramp signal was applied to the positive input of the headstage amplifier (Analog Devices, ADA4062-4ACPZ-R7) while the negative input was connected to the carbon fiber electrode (Takmakov et al., 2011). The amplifier was powered with ± 15 V (B&K Precision, 1672) and had a gain of 200 nA/V with the use of a 4.99 MΩ resistor. The output of each amplifier was fed into one of the analog inputs' positive terminals on the R series cards (i.e., one fiber per analog input). The ramp signal that was applied to the amplifiers was also sent directly to the same analog inputs' corresponding negative terminals. The differential of these two signals is the measured signal.

Connecting the R series cards to the headstage used a variety of adapters and interfaces. Briefly, from the R series cards SHC68-68-RMIO cables (National Instruments) were connected to a custom interface box. The output of this box was a DB25 connector that was interfaced to an Omnetics A79029-001 connector (Omnetics Connector Corporation) using a 24-conductor wire bundle (Digikey, MB24S-50-ND). The A79029-001 connector mated with the headstage which had connector A79024-001 from Omnetics.

The acquisition software was written in LabVIEW (National Instruments) and acquired 1000 points of data during each ramp signal. Each channel had its data saved to separate files in 30 sec increments; however, this value can be changed based on experimental needs. If enabled, the software generated a stimulation trigger signal that was routed through another analog output of the first R series card. This trigger signal was then routed to a stimulus isolator that delivered a stimulation current to an implanted stimulating electrode. The stimulation trigger signal was programmed to be applied during the -0.4 V hold period, so as not to interfere with data acquisition during the ramp period.

A complete guide to the system's hardware and software specifications can be found at https://chestekresearch.engin.umich.edu/carbon-fibers/.

HDCF Array (Working Electrode) Calibration

To provide calibration data, the 16-channel HDCF array (Huan et al., 2021) functionalized with 50 µm laser-ablated tip sites and treated with plasma ashing (Patel et al., 2020) was lowered into a flowcell that was constructed in house. Artificial cerebrospinal fluid (aCSF) (125 mM NaCl, 1.3 mM $CaCl_2$, 4 mM KCl, 2.66 mM PO_4, 1 mM KCl_2) made with 3x filtered water and brought to a pH = 7.2-7.4, was kept at a constant flow rate of 100 mL/hr. A chemical reference was provided by a silver | silver chloride (Ag|AgCl) reference electrode. The reference electrode was made by submerging one end of a silver wire (Sigma, 265 586) in 2N hydrochloric acid (HCl) (ThermoFisher, SA431500) while the other end was connected to the cathode end of a power supply. A silver wire from the same manufacturer, also submerged in the HCl, was connected to the anode end of the power supply. The power supply was set to 5 V and turned on for 30 sec.

The device was first cycled at a rate of 60Hz for 5-10 min and then 10Hz for 30 min. This 'cycling session' stabilizes the working electrode signal. The device was then pulsed with 3 bolus each of 4 different concentrations of dopamine hydrochloride (Sigma, H8502-10G), 0.5 µM, 1 µM, 2 µM, and 4 µM, in aCSF at 250 mL/hr. During the dopamine oxidation period values were measured at three times, at the peak of the onset, just before the falloff from the washout, and then in between these two times. The obtained measurements were then averaged into a calibration curve for the devices per cohort. The fiber tips were dipped and held in 3% hydrogen peroxide for 7 seconds and then isopropyl alcohol for 7 seconds to clean the carbon fiber surface and remove any contamination that had bonded to the carbon (Patel et al., 2020). Devices were sterilized with ethylene oxide.

Experiment 1, Part A: Fast-Scan Cyclic Voltammetry Surgery in the NAc

Male and female rats were anesthetized with a combination of ketamine (60 mg/kg, i.p.) and dexmedetomidine hydrochloride (0.3 mg/kg i.p.). A 3-arm stereotaxic apparatus was used with custom multiangle device holders. The first opening through the skull was made for the Ag|AgCl reference electrode cannula in the contralateral cortex from the working electrode coordinates. A second opening was made in the skull at the site for implantation of the stimulating electrode. A third opening was made in the skull centered over the working electrode coordinates to form a 2.8 mm x 1.4 mm oval. Next, holes were drilled along the perimeter of the incision site for 6-8 bone screws (Grainger, 1ZA99) to secure the devices to the skull. Screws are

hand-driven into place, and then a layer of Metabond dental adhesive (Henry Schein, 1865548) was added, making sure to thoroughly coat each of the skull's screws while avoiding openings created for the three electrodes. Next, the dura was resected while preserving the cortex. Blood and cerebrospinal fluid were absorbed with eye spear surgical sponges (Henry Schein, 1245120).

A reference electrode cannula (BASi, MD-2251), was trimmed 5 mm below the pedestal. Next, the Ag|AgCl wire was glued into the cannula's mating connector and inserted into the cannula, extending 2 mm past the end of the trimmed tube. An acute reference electrode in the cannula was lowered into position (AP -3.0 mm, ML ±3.5 mm, DV (relative to the skull) -1.2 mm). A bipolar stimulating electrode (Plastics One, Inc., MS303/2-B/2 ELEC .008" TW Bend 6.5 mm over, 12 mm after bend) was lowered from the top of the skull into the ventral tegmental area (VTA) (AP -5.15-5.2 mm, ML ±0.75-0.8 mm, DV (relative to the skull) -8.2-8.4 mm). The working electrode's fiber tips were brought to the brain surface and the FSCV system was turned on. The stimulating electrode was lowered 0.2 mm every 10 sec, while the HDCF array was slowly lowered 0.1 mm every 10 sec from zero, which was the top of the brain into the NAc (AP +1.35-1.4 mm, ML ±2.9-3.2 mm, DV (relative to the cortical surface) -6.8-7.2 mm, at an angle of 16.7 degrees). Unlike more rigid electrodes, the flexible carbon fibers can be deflected by the tough epithelial cells of the lateral ventricles when targeting the medial region of the NAcS. To avoid this problem the electrodes were implanted at an angle. A stimulus isolator was used to apply stimulation pulses to the stimulating electrode using the custom LabVIEW software. These stimulation pulses were used to stimulate DA release for detection by the working electrode once in place.

Electrodes were anchored in place with the use of dental acrylic. The working and stimulating electrodes were covered with protective dust caps (Omnetics, A79041-001 and Plastics One, Inc., 303DCMN) and the reference electrode cannula was occluded with the provided sterile stylet. At the conclusion of the surgery, rats were given atipamezole hydrochloride (0.5 mg/kg i.p.) and dexamethasone (200 µg/kg s.c.). The rats then went through standard post-operative care.

Experiment 2, Part A: Fast-Scan Cyclic Voltammetry Surgery in the DLS

The surgery protocol was the same as previously described. Coordinates were modified for the DLS for the working electrode and the stimulating electrode was implanted into the medial forebrain bundle (MFB). Coordinates in relation to bregma: working electrode targeting

the DLS: (AP +0.2 mm, ML ±3.0 mm ± 1.0 mm, DV (relative to the cortical surface) -4.0 mm), bipolar stimulating electrode (Plastics One, Inc.) targeting the MFB: (AP -1.8 mm, ML ±2.0 mm ± 0.5 mm, DV (relative to the skull) -7.8 mm for males and -7.5 mm for females), and reference electrode guide cannula in the contralateral cortex (AP -3.0 mm, ML ±3.5 mm, DV (relative to the skull) -1.2 mm).

Experiment 1, Part B: Fast-Scan Cyclic Voltammetry Testing (NAc)

On day 11 post-surgery, animals went through a cycling session where an Ag|AgCl reference electrode was lowered into the reference electrode cannula and a headstage was connected to the working electrode. The stimulating electrode was connected to the isolation unit. The reference electrode was connected to the headstage using a gold pin connector. The working electrode was repeatedly cycled at a rate of 60Hz for 10-15 min or until the detected current was stable for 5 min. The waveform was then cycled at a rate of 10Hz for 20-30 min or until the standard deviation for the detected current was consistently below 0.4 nA for 5 min. This 'cycling session' stabilizes the working electrode signal. On testing days, a cycling session occurs before any recordings are taken, then a 10 min baseline recording is collected with the applied waveform repeatedly cycled at a rate of 10Hz. All data recordings were collected at 10Hz. Following the baseline collection, three 30 sec stimulation events recordings were taken, with 3-5 min between each recording. Five seconds into each recording, a pulse train was applied to the stimulating electrode using a stimulus isolator controlled by custom LabVIEW software. For our stimulation events, three stimulation parameters were used: pulse trains of 30Hz 15 total pulses (p), 60Hz 30p, or 60Hz 60p. During the initial stimulation test session, the peak amplitude of the current applied was optimized for each rat, ranging from 120-200 µA, and held constant for all pulse trains (Example stimulation parameter: 30Hz 15p, 60Hz 30/60p 150 µA). Animals were monitored during each stimulation trial and their physical reactions were recorded. Following the last stimulation event, the working and stimulating electrodes were disconnected from their respective cables and hardware, and their dust caps replaced. The reference electrode was removed and replaced with a sterile stylet.

Experiment 2, Part B: Fast-Scan Cyclic Voltammetry Testing (DLS)

The cycling session followed the same procedure as described above and animals were tested during the beginning of their light/dark cycle. The testing days followed the same procedures for initial cycling and collection of baseline recordings as described above, but with

different stimulation parameters. For our stimulation events the parameters were as follows, 60Hz 30p, 60Hz 60p, or 60Hz 120p. During the initial stimulation test session, the peak amplitude of the current applied was optimized for each rat, ranging from 90-150 µA, and held constant for all pulse trains (Example stimulation parameter: 60Hz 30/60/120p 150 µA). Data presented here are prior to other experimental manipulations.

Data Processing

All FSCV data was collected and stored as UTF-8 int16 and analyzed using chemometric analysis with principal component regression (PCR). In preprocessing, each CV was filtered through a 4th order, 2 kHz low pass infinite impulse response (IIR) filter to remove non-biologically relevant noise (Montague et al., 2004). A zero-phase 2nd order, 0.01 Hz high pass Butterworth IIR filter was used on each potential step across time to remove background drift due to charging current (DeWaele et al., 2017).

Figure 1. Experimental flow diagram and setup. **A,** Experimental flow and time course for each cohort of animals. **B,** Experimental setup for all animals. Electrodes were either implanted in the NAc or DLS. During behavioral experiments, animals were connected to the acquisition system via a headstage and cable.

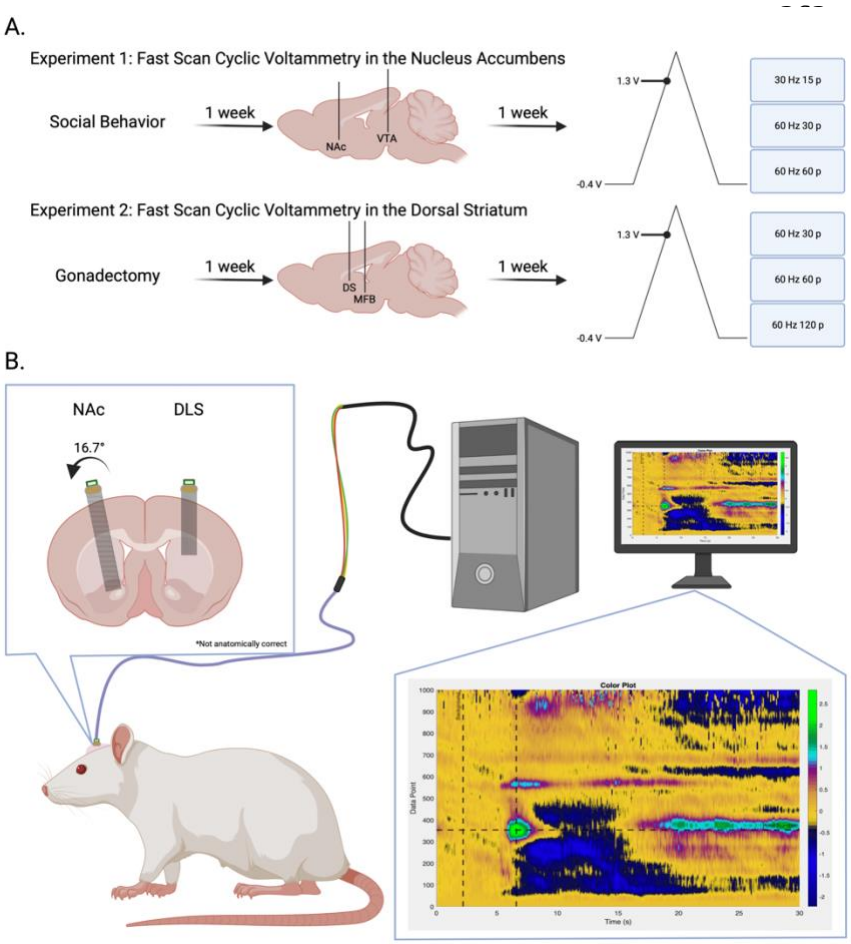

PCR was performed using in-house MATLAB code. A standard training set was constructed based on *in vivo* recordings. Current was converted to concentration using the electrode calibration factor obtained before implantation. If the calculated concentration for a channel fell outside of the mean of all 16 channels ± 2 standard deviations, it was identified as an outlier and removed. The training set

consisted of 5 DA, 3 acidic pH, and 2 basic pH voltammograms. Voltammograms were collected from multiple animals while implanted in either the DLS or NAc.

Code Accessibility

Custom MATLAB code is available from the corresponding author upon request.

Experimental Design and Statistical Analysis

All statistical analyses were performed using GraphPad Prism v9.0

Experiment 1: NAc

Data was analyzed using ANOVA to look at the effects of maximum increase in DA (mean max DA; defined as the difference between pre-stim baseline and the peak height [DA] (nM) within 10 sec of the stimulation pulse) of group effects during baseline in the NAcC and NAcS. To look at significant differences, the Tukey's comparison's test was used.

Experiment 2: DLS

A Geisser-Greenhouse correction was used because sphericity was not assumed. The threshold for significance for all statistical tests was set to $p < 0.05$. A two-way ANOVA was conducted to assess differences in ES DA release within a specific pulse parameter (60Hz 30/60/120p) across time. Two-way ANOVAs were also used to assess sex differences in Tau, a measure of DA reuptake, across time. In the case of a significant interaction, a Šídák correction was used for multiple comparisons.

Histology - Sectioning

In order to maintain placement of individual electrode fibers, the skull was extracted with the implant intact and sectioned using a slice-in-place technique (Patel et al., 2020). Briefly, animals were sedated with Fatal Plus (Vortech Pharmaceuticals, V.P.L. 9373) and transcardially perfused with 0.1 M phosphate buffered saline (PBS) followed by 4% paraformaldehyde (ChemCruz, SC-281692). The animal was then decapitated, and the skull was stripped of skin, ensuring the implant remains cemented to the skull. The skull was then soaked in 0.25 M ethylenediaminetetraacetic acid (Sigma, E5134) in 0.1 M PBS solution at 4 °C with low agitation. The solution was changed every 24 hours for 14 days. The softened skull was then transferred into a 30% sucrose (Sigma, S0389) solution with 0.02% sodium azide (Sigma, S2002) for 48 hours or until sectioning. Before sectioning, skulls were immersed in OCT

(ThermoFisher, 4585) and put under a -0.06 MPa vacuum. Skulls were frozen and mounted on a cryostat (ThermoFisher, HM 525NX). 300 μm horizontal sections were taken at -19 °C and stored in 0.1 M PBS with 0.02% sodium azide.

Histology - Immunohistochemistry

Staining protocols were adapted from Patel et al., 2020. All steps were done under low agitation conditions. Sections were selected for histology by visual verification of carbon fiber tips in tissue with an optical stereo microscope (Amscope SMZK-1TSZ, WF 10x/20). Sections were incubated in 4% paraformaldehyde at 4 °C for 24 hours, then given two 1 hour, 1x PBS washes followed by incubation in Starting Block blocking buffer (ThermoFisher, 37538) with 1.5% Triton X-100 (Sigma, 93443) for 24 hours at room temperature. The sections were then washed in 1x PBS with 0.5% Triton X-100 (PBST) three times, 1 hour per wash, and incubated in a primary antibody cocktail containing mouse anti-NeuN (Millipore, MAB277 lot 3574318, 1:500 dilution), chicken anti-tyrosine hydroxylase (TH) (Abcam, AB76422 lot GR3367897, 1:500 dilution), rabbit anti-calbindin (CB) (Swant, CB-28a lot 9.20, 1:500 dilution) or rabbit anti-μ-opioid receptor (M-OR) (Immunostar, #24216 lot 20290001, 1:500 dilution) in 1.5% Triton X-100, 0.02% sodium azide, and 1% donkey serum for 10 days at 4 °C. Following three more 1 hour washes in 0.5% PBST, sections were incubated with secondary antibodies donkey anti-mouse Alexa 647 (Jackson, 715-605-150, 1:500 dilution), anti-chicken Alexa 488 (Jackson, 703-545-155, 1:500 dilution), anti-rabbit Alexa 546 (Life Technologies, A10040, 1:500 dilution), DAPI (Invitrogen, D1306, 1:2000 dilution), 0.5% Triton X-100, 0.02% sodium azide, and 1% donkey serum for 4 days at 4 °C. Finally sections were washed twice, 2 hours each wash, in 0.5% PBST and then stored in 1x PBS with 0.02% azide.

Histology - Imaging and Analysis

Sections were imaged on a Zeiss LSM 780 confocal microscope using a 10x objective (Zeiss, C-Apochromat 10x/0.45 W M27). Sections were cleared by immersion in 80% 2,2'-thiodiethanol (TDE) (Sigma, 88561) for 45 minutes to 1 hour and mounted on electrostatic slides with slide spacers containing TDE. The active surface of the working electrodes is a cylinder with a height of ~50 μm and a diameter of approximately 6.8 μm. A z-stack image containing the full 16 fibers with 8 μm steps was used to locate each electrode tip. Images were analyzed using the Fiji distribution of ImageJ (Schindelin et al., 2012).

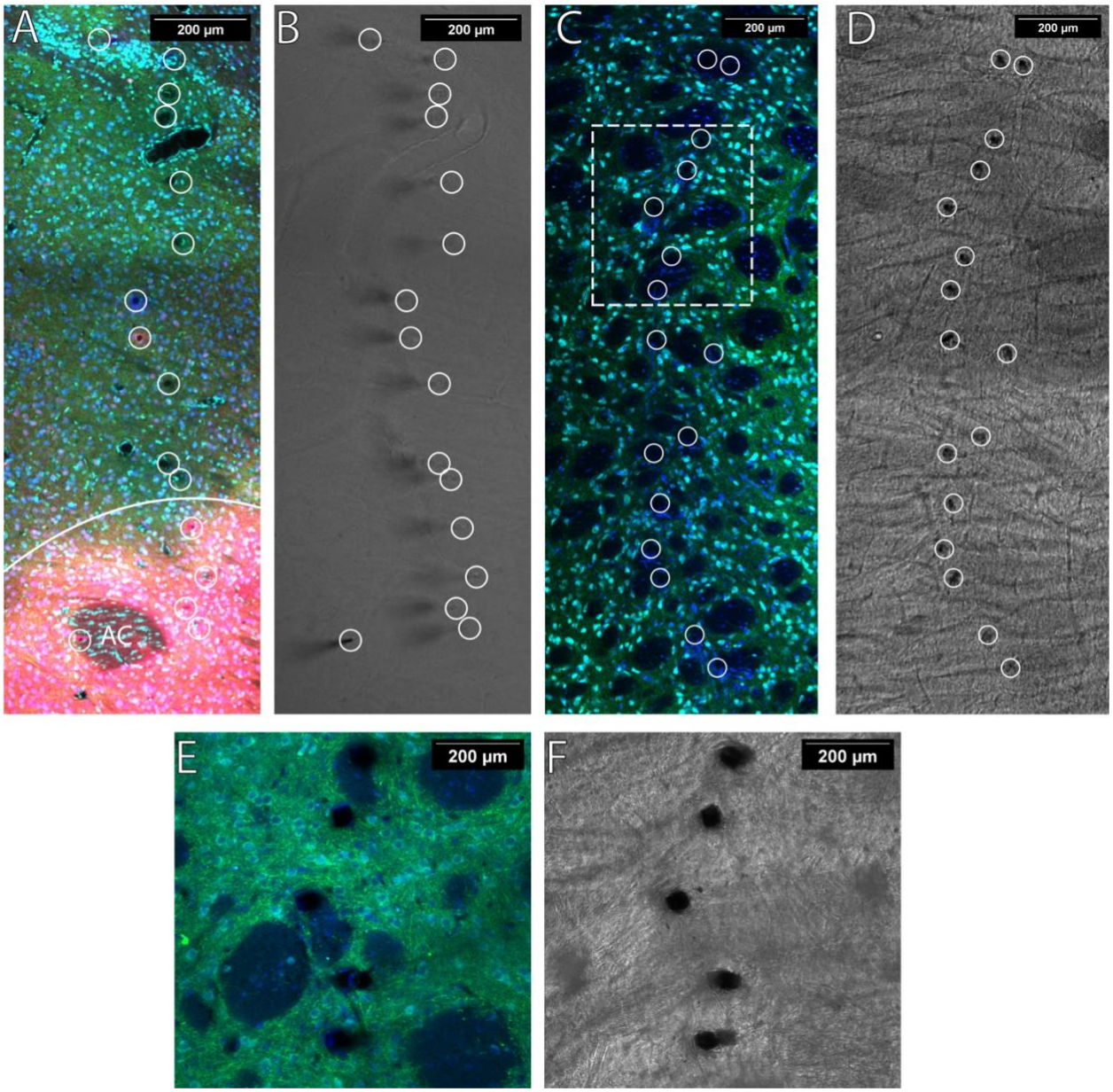

Figure 2. Fiber locations were verified with widefield imaging and placements are indicated with white circles. TH (green) indicates electrode fibers are placed in DA containing regions. **A,** When imaging the NAc, Calbindin (red) was used to determine NAcC versus NAcS delineated by the solid white line**.** The anterior commissure is denoted AC. NeuN (cyan) and DAPI (blue) were used to infer if electrode fibers were placed in a region containing neuronal cell bodies. **B,** Representative widefield image of tissue presented in A. **C,** Image with electrode embedded in the DLS with **D,** corresponding widefield image **E,** A close up image of five representative electrode locations of the same tissue present in panel C with it's corresponding widefield image. The contrast of all widefield images were adjusted using the built-in enhance contrast function to Fiji to assist in viewing.

Electrodes targeting the NAc were placed in either the NAcC or NAcS subregions. The NAcC was defined as TH+ and CB+ with strong nuclei and neuropil (Fig. 2A). The NAcS was

defined as TH+ and CB- and lateral to the olfactory tubercle or the slight CB+ border region directly flanking the NAcC. When sectioning extracted tissue horizontally the individual electrodes terminate in different DV planes. If more than 8 μm of an electrode was placed in the NAcC or on border regions between the NAcC and NAcS, then the electrode was classified as being located in the NAcC. If more than 24 μm of the active electrode surface was TH- or fell into the olfactory tubercle they were excluded from the analysis.

Representative image showing staining for TH, NeuN, and DAPI in the DLS as illustrated in Figure 2B.

While not highlighted in this paper, regions of the striatum such as the DLS are highly heterogeneous, composed of both patch and matrix compartments (Brimblecombe and Cragg, 2017). These electrodes could also be used to more closely examine differences between the two, by comparing the measurements of fibers after verifying their placements using our histological methods.

Results

Experiment 1: Nucleus Accumbens – Effect of Social Housing

Electrodes were identified postmortem as being in the core or shell as described in the methods. Overall, pair - housed females had a higher ES Δ[DA] (nM), compared to single housed females in the NAcC at 60Hz 30p and 60Hz 60p (one-way ANOVA; Figs. 3A & 3B). There were no differences among groups in the NAcS (Figs. 3C & 3D).

When looking at the NAcC (Fig. 3A), pair - housed females had significantly higher ES Δ[DA] release compared to the single females ($p < 0.0001$). Pair - housed females also had higher ES Δ[DA] release compared to male singles ($p = 0.0407$) and pair - housed males ($p = 0.0154$). At 60Hz 60p, pair - housed females had significantly ES Δ[DA] release compared to the single females ($p < 0.0322$). In the NAcS, there were no significant group differences found at 60Hz 30p and 60Hz 60p.

Figure 3. NAc DA release across subregions. **A,** ES DA in the NAcC after stimulation using 60Hz 30p. Here we found that there was a group effect (($F(3, 159) = 7$; $p < 0.0001$)). pair - housed females had significantly higher ES DA compared to the single females. pair - housed females had higher ES DA compared to male singles ($p = 0.0407$) & pair - housed males ($p <$

0.0154). **B,** Mean max DA in the NAcC after stimulation using 60Hz 60p. Here we found that there was a group effect ((F(3, 158) = 7; p = 0.0347)). pair - housed females had significantly higher ES DA compared to the single females. **C,** ES DA in the NAcS after stimulation using 60Hz 30p. No significant effects were found. **D,** ES DA in the NAcS after stimulation using 60Hz 60p. No significant effects were found. Data points indicate values from individual fibers. Bars shown indicate standard error of the mean (SEM). *p < 0.05, ****p < 0.0001

Figure 3. NAc DA release across subregions. **A,** ES DA in the NAcC after stimulation using 60Hz 30p. Here we found that there was a group effect ((F(3, 159) = 7; p < 0.0001)). pair - housed females had significantly higher ES DA compared to the single females. pair - housed females had higher ES DA compared to male singles (p = 0.0407) & pair - housed males (p < 0.0154). **B,** Mean max DA in the NAcC after stimulation using 60Hz 60p. Here we found that there was a group effect ((F(3, 158) = 7; p = 0.0347)). pair - housed females had significantly higher ES DA compared to the single females. **C,** ES DA in the NAcS after stimulation using 60Hz 30p. No significant effects were found. **D,** ES DA in the NAcS after stimulation using 60Hz 60p. No significant effects were found. Data points indicate values from individual fibers. Bars shown indicate standard error of the mean (SEM). *p < 0.05, ****p < 0.0001

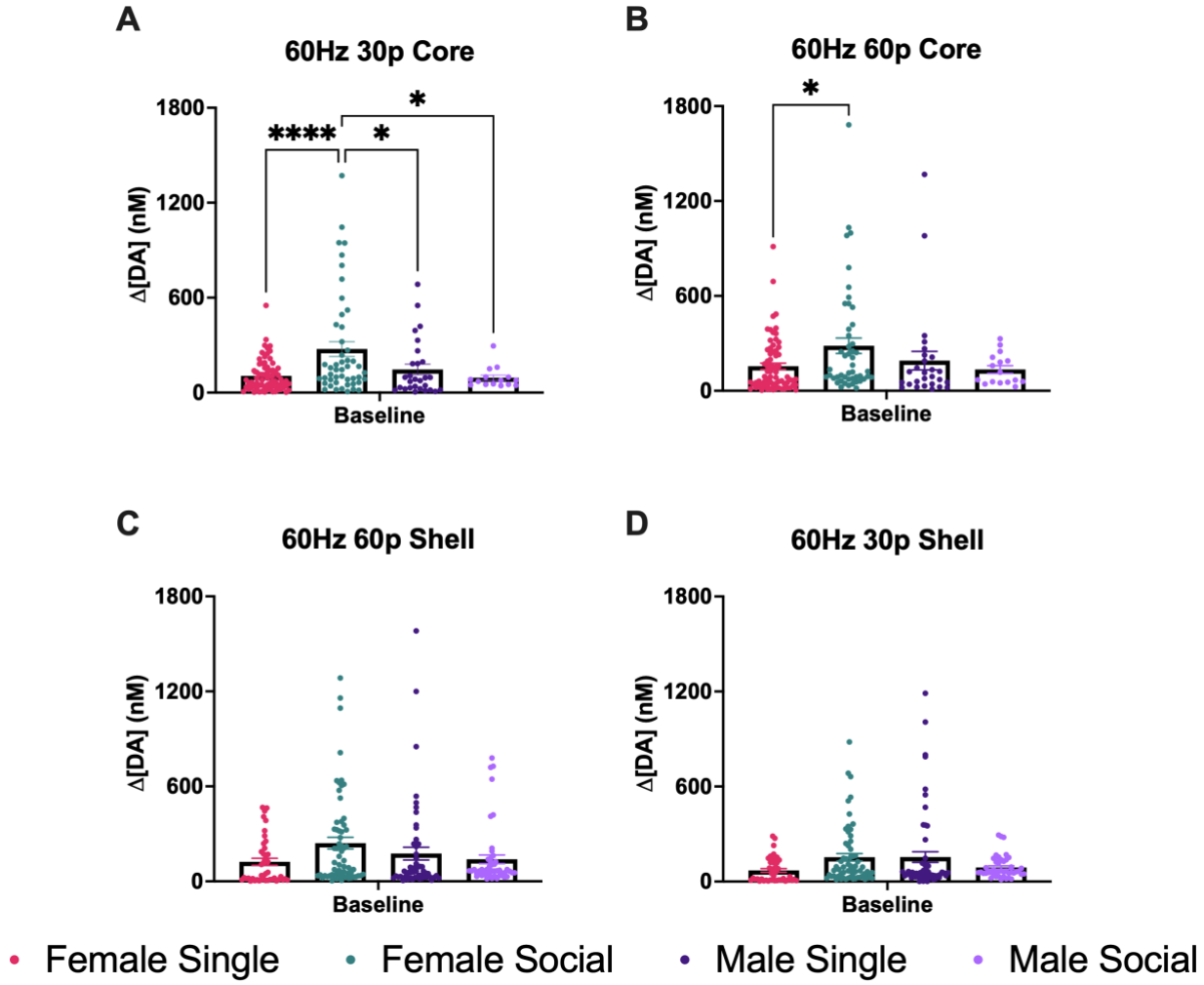

A two-way ANOVA was conducted to examine differences between NAcC and NAcS between groups. Overall, pair - housed females had a higher ES Δ[DA] release in the NAcC compared to the NAcS ($p = 0.0034$) at 60Hz 30p (Fig. 4A). No other group differences were found. There were no group differences found at the 60Hz 60p stimulation parameter (Fig. 4B). Thus, housing conditions differentially affected ES Δ[DA] release in the NAcC core of female rats.

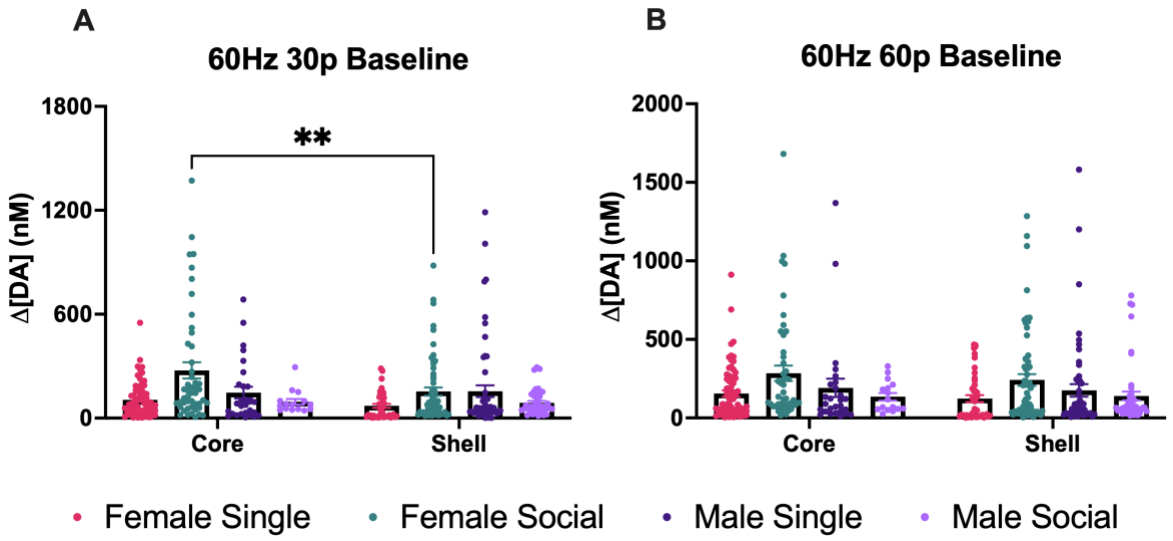

Figure 4. The graphs show the comparison between brain regions within groups at two different parameters. **A,** The graphs show differences between NAcC and NAcS at 60Hz 30p. Pair-housed females had higher ES DA release in the NAcC than the NAcS ($p < 0.003$). **B,** No significant differences were found. Data points indicate values from individual fibers. Bars shown indicate SEM. $^{**}p < 0.01$

Experiment 2: DLS shows a significant enhancement in ES-induced DA release with repeated ES in both males and females.

ES DA release, Δ[DA] (nM), was assessed at three stimulation parameters across four weeks. Stimulation parameters, as well as the timing between stimulations, were picked to minimize carry-over effects on DA release between recordings.

ES DA release, Δ[DA] increased significantly over time in both castrated (CAST) males (Fig. 5A) and ovariectomized (OVX) females (Fig. 5B). In both OVX and CAST ES-induced DA release in DLS was enhanced as a function of repeated stimulation. Color plots of DA

release from each of the 16 channels of one rat over 4 weeks is illustrated this increase in Figure 6.

There were no sex differences in ES DA release at any stimulation parameter. On the other hand, for Tau (ms), a measure of DA reuptake, there was significant effect of sex ($p = 0.0001$), as well as a significant sex X week interaction ($p = 0.0037$). Overall, Tau was greater in OVX females compared to CAST males across the four weeks (Fig. 7) indicating slower reuptake in OVX rats. There was no overall effect of time on Tau, indicating sensitization of DA release occurred independent of the sex differences in DA reuptake.

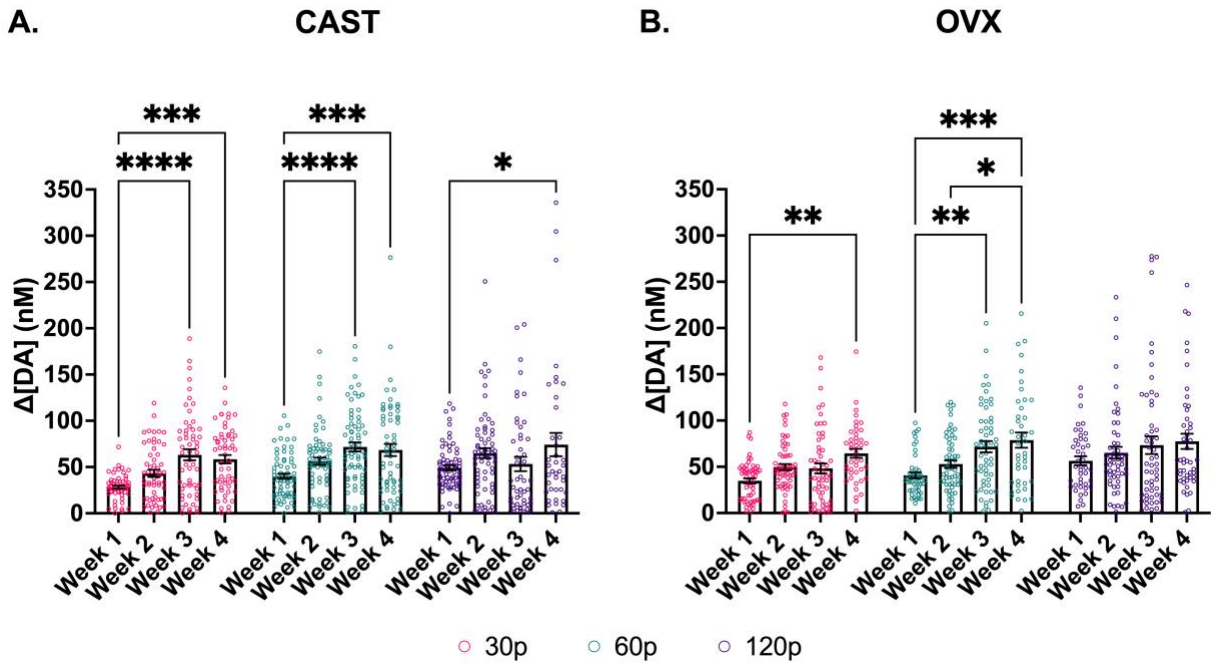

Figure 5. Electrically stimulated DA release increases across time in both CAST and OVX rats. **A,** In CAST males, there was a significant effect of pulse number ($F(2, 713) = 6.11$; $p = 0.0023$) and week ($F(3, 713) = 16.34$; $p < 0.0001$), as well as an interaction between pulse number and week ($F(6, 713) = 2.22$; $p = 0.0391$). Multiple comparisons revealed a significant difference between week 1 and weeks 3 ($p < 0.0001$) & 4 ($p = 0.0005$) at the 30 pulse parameter. There was also a strong trend toward significance between weeks 2 & 4 ($p = 0.0510$). At the 60 pulse parameter there were significant differences between week 1 and weeks 3 ($p < 0.0001$) & 4 ($p = 0.0005$). For the highest stimulation parameter there was a significant difference between weeks 1 and 4 ($p = 0.0114$). **B,** In OVX females, there was a significant effect of pulse number ($F(2, 610) = 10.22$; $p < 0.0001$) and week ($F(3, 610) = 12.24$; $p < 0.0001$), but no interaction between pulse number and week. Multiple comparisons at the lowest stimulation parameter revealed a significant difference between weeks 1 and 4 ($p = 0.0036$). At the 60Hz 60p, multiple comparisons revealed significant differences between week 1 and weeks 3 ($p = 0.0018$) & 4 ($p = 0.0002$) as well as between weeks 2 and 4 ($p = 0.0180$). Data points indicate values from individual fibers. Bars shown indicate SEM. *$p < 0.05$, **$p < 0.01$, ***$p < 0.001$, ****$p < 0.0001$, significantly different between weeks.

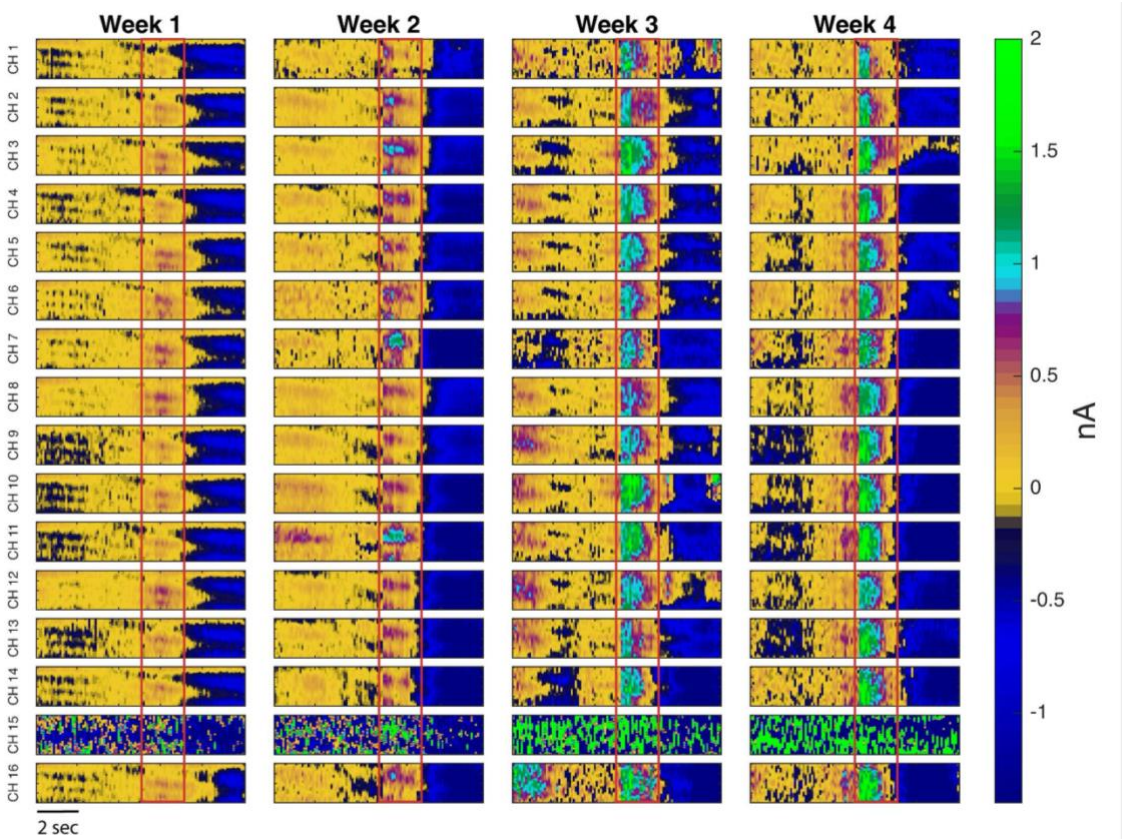

Figure 6. Representative false color plots of DA release in the DLS of one male rat, #1M, over four weeks. The red box denotes the onset and conclusion of a 60Hz 120p stimulation train. As can be seen from this color plot the Δ[DA] (nM) response increased over four weeks. In this particular animal channel 15 malfunctioned, but channels 14 and 16 functioned as expected.

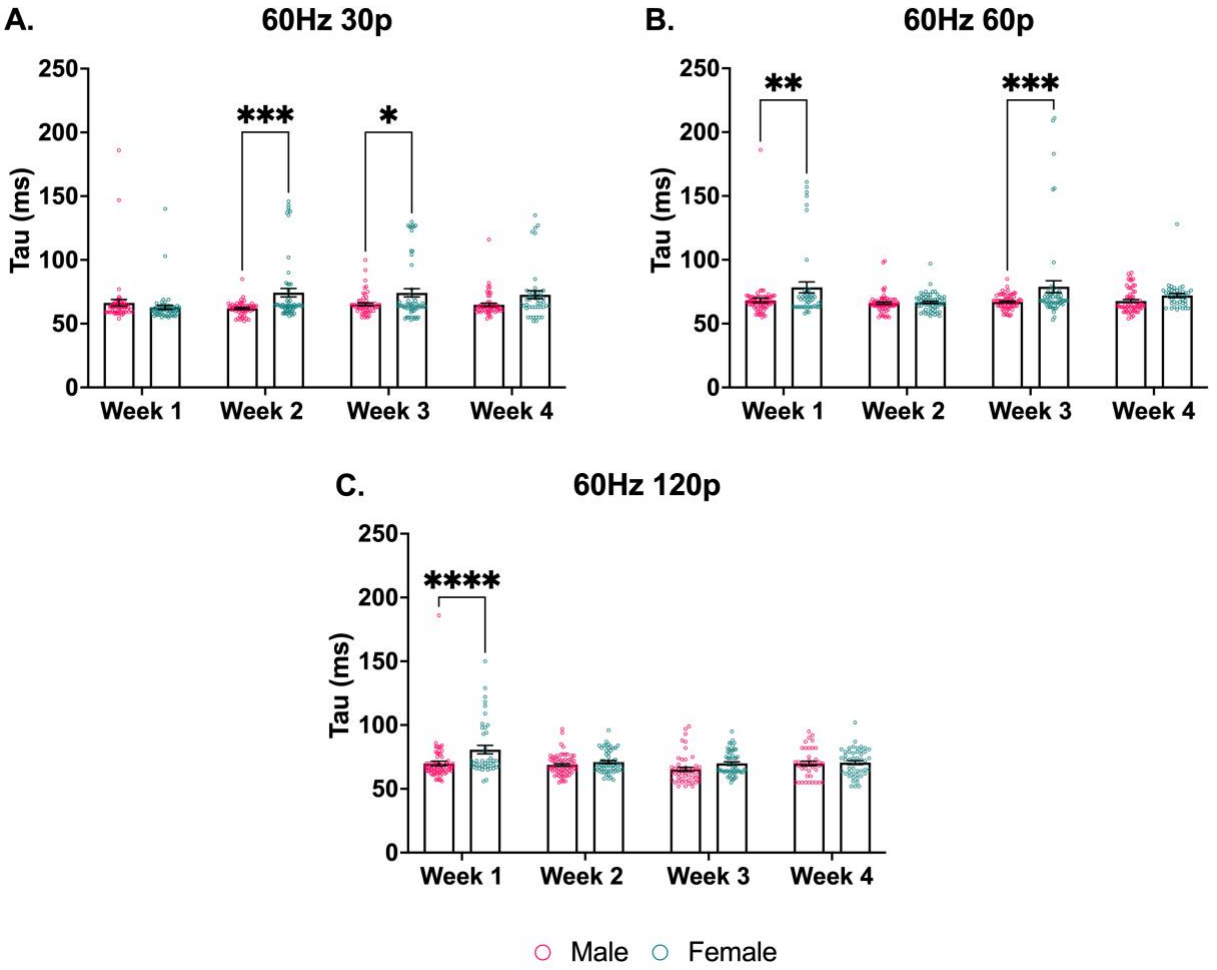

Figure 7. Sex differences in Tau. **A,** At the lowest stimulation parameter, there was a significant effect of sex ($F(1, 437) = 15.23$; $p = 0.0001$)), as well as a significant interaction between sex and week ($F(3, 437) = 4.55$; $p = 0.0037$), but no effect of week. Multiple comparisons revealed significant differences between males and females during week 2 ($p = 0.0005$) and week 3 ($p = 0.0238$). **B,** At the 60Hz 60p stimulation parameter, there was a significant effect of sex ($F(1, 461) = 17.57$; $p < 0.0001$)), and week ($F(3, 461) = 4.28$; $p = 0.0054$) as well as a significant interaction between sex and week ($F(3, 461) = 2.74$; $p = 0.0427$). Multiple comparisons revealed significant differences between males and females during week 1 ($p = 0.0074$) and week 3 ($p = 0.0007$). **C,** At 60Hz 120p, there was a significant effect of sex ($F(1, 423) = 14.22$; $p = 0.0002$) and week ($F(3, 423) = 7.05$; $p = 0.0001$) as well as an interaction between sex and week ($F(3, 423) = 3.30$; $p = 0.0203$). Multiple comparisons revealed significant differences between males and females during week 1. Data points indicate values from individual fibers. Bars shown indicate SEM. ($p < 0.0001$). *$p < 0.05$, **$p < 0.01$, ***$p < 0.001$, ****$p < 0.0001$.

Discussion

For the first time we show that housing conditions can differentially affect ES DA release in the NAcC vs NAcS when recorded simultaneously from these brain regions of female rats. Housing conditions did not affect stimulated DA release in males. We also demonstrate sensitization of ES DA release longitudinally using this novel 16-channel electrode recording in the DLS over 4 consecutive weeks. In both CAST males and OVX females ES DA release increased significantly over time. With this chronically implanted electrode, we were able to look at differences in ES DA release within regions and across weeks and see sex-related differences in both the NAc and DLS.

In the NAcC we found that pair-housed females had a higher ES DA release compared to single housed females at both stimulation parameters. At 60Hz 30p, pair - housed females had a higher ES DA release compared to single housed males and pair-housed males. Pair-housed females have higher ES DA release in the NAcC compared to single housed females. These data show us that social housing conditions of the females influence the ventral tegmental area DA neuron responsivity to ES. Previous findings from this laboratory have found that singly housed females had a greater methamphetamine-induced increase in DA from the NAc (core and shell) compared with pair-housed females using in vivo microdialysis (Westenbroek et al., 2019). Differences in the methods for measuring and stimulation of DA release certainly contribute to the differences in the direction of the findings. FSCV measures rapid dynamic changes in DA release and isolated NAcC vs. NAcS while microdialysis sums effects on DA release, reuptake and diffusion over ten min. Nevertheless, the two studies demonstrate that housing conditions in female rats affect dynamic DA responses to stimulation.

Previous studies have shown that social isolation does not have an effect on DA basal levels in male rats in NAc, using microdialysis (Novoa et al., 2021) and this is consistent within our findings. Social isolation increased ES-induced DA release in NAc, using FSCV, in adult male mice, but this report did not find an effect of housing in adolescence males (McWain et al., 2022). In our studies males were pair-housed from adolescence, but FSCV recording occurred in adults.

While most studies have only looked at male subjects, other studies which looked at males and females found that social housing had a positive effect for females but not males in

relation to coping with stress (Westenbroek et al., 2003). Previous studies also showed that social housing attenuates drug self-administration in females, but not in males (Westenbroek et al., 2013; Lee et al., 2017; Moench and Logrip, 2021).

Studies looking at mice showed that social hierarchies vary in a sex-dependent manner. For example, male dominance remains stable and robust over time while females' social hierarchy is less rigid (Karamihalev et al., 2020). In a study looking at monkeys, dominant female monkeys had higher D2/D3 receptor availability compared to paired subordinate monkeys (Nader et al., 2012). In our study, the animals that underwent the FSCV surgery and testing were the dominant of the pair and this could be a potential reason for the social females having higher ES DA release. Further studies need to be conducted using both subordinate and dominant females. These results show us a potential way that social housing is playing a role in NAc activity.

In vitro, phasic DA release in the ventral striatum has been reported to vary between NAcC and NAcS in female mice (Brundage et al., 2022). Here we see that with both single housed females and pair - housed females there was a significant difference in the NAcC but not the NAcS, consistent with what previous studies have shown. Further studies should be conducted to better understand the differences between the regions.

In the DLS, our results showed that ES DA release increased from week one to week four at both the 60Hz 30p and 60p stimulation parameters in both CAST and OVX, providing evidence for sensitization across time. These findings are supported by other work looking at DA release in the DLS. Amphetamine administration has been shown to induce time-dependent enhancement of DA transmission in dorsal striatum, compared to saline pretreatment, using microdialysis (Paulson and Robinson, 1995). The previous study used one-time measurements after either 3, 7, or 28 days of withdrawal from amphetamine. Only animals tested after 28 days of withdrawal showed a significant enhancement in amphetamine-induced DA release as measured using in-vivo microdialysis (Paulson and Robinson, 1995).

Previous data from the laboratory has shown sex differences in basal DA levels in the dorsal striatum of gonadectomized male and female rats, with CAST males having significantly greater basal levels (Castner et al., 1993; Xiao and Becker, 1994; Cummings et al., 2014). However, it is essential to note that previous studies were conducted using microdialysis, which has a much lower temporal resolution, ~5-10 minutes, compared to the sub second resolution of

our carbon fiber electrodes. These differences in basal levels could be attributed to differences in DA release, reuptake, diffusion or a combination. The current study looked at dynamic responses to stimulation rather than basal release.

In the DLS of gonad-intact females, the DA active transporter (DAT) is more active and present in higher concentrations (Rivest et al., 1995; Walker et al., 2000; Dluzen and McDermott, 2008). Across several minutes, DA concentrations may appear to be relatively lower in females than males due to higher rates of reuptake. With a higher temporal resolution, we can make more nuanced observations. Such as in this study we saw that Tau was higher in females than males, suggesting lower DA reuptake in OVX females compared to CAST males. Studies to investigate the effects of ovarian hormones on Tau are in progress.

While we saw sex differences in the effect of housing conditions in the NAcS, those animals were gonadally intact. The animals used for our DLS experiments were gonadectomized, possibly explaining our lack of more prominent sex differences. Circulating hormones are known to play a significant role in modulating DA signaling in the DLS (Robinson and Becker, 1982; Hu and Becker, 2003; Cummings et al., 2014; Song et al., 2019). One study demonstrated that OVX animals show upregulation of DAT in the absence of estradiol (Attali et al., 1997). An FSCV study found that DA release and reuptake in the DLS are greater in intact females than intact males (Walker et al., 2000). Future studies will examine intact animals to determine whether we can replicate these findings.

Conclusion

Our findings provide evidence that housing conditions modulate ES DA release in the NAc in a region- and sex-dependent manner. Furthermore, repeated ES causes sensitization of DA in the DLS of both males and females, as indicated by enhanced ES DA release across weeks. The data also suggest that sex significantly affects DA reuptake in the DLS, with OVX females having lower DA reuptake levels than CAST males. Our results also demonstrate the viability of these electrodes to chronically detect DA release from multiple locations in subregions of the striatum of freely moving rats. We successfully monitored DA release in the NAcC and NAcS simultaneously with a single device and DA release in the DLS over 4 weeks.

The implications of these results are far-reaching. DA signaling within and between these striatal regions has been consistently tied to learning, motivated behaviors, and addiction vulnerability. Differences between males and females are also believed to be a primary driver for

sex differences in escalation of addiction-like behavior (Quigley et al., 2021). However, assessing dynamic changes in these regions over time reliably has proven difficult, especially in freely moving subjects. The unique combination of high temporal and spatial resolution provided by these novel electrodes opens numerous exciting avenues for future research as we can better study the role of these highly dynamic and heterogenous populations of neurons in motivated behavior and any sex differences therein.

Acknowledgements: These experiments were supported by grants from the USPHS: NIH R01DA049795 & R01DA046403 to JBB; UF1NS107659 to CAC; NIDAT32 pre-doctoral Training Program in Neuroscience

References

Attali G, Weizman A, Gil-Ad I, Rehavi M (1997) Opposite modulatory effects of ovarian hormones on rat brain dopamine and serotonin transporters. Brain Res 756:153–159.

Brimblecombe KR, Cragg SJ (2017) The Striosome and Matrix Compartments of the Striatum: A Path through the Labyrinth from Neurochemistry toward Function. ACS Chem Neurosci 8:235–242.

Brundage JN, Mason CP, Wadsworth HA, Finuf CS, Nelson JJ, Ronström PJW, Jones SR, Siciliano CA, Steffensen SC, Yorgason JT (2022) Regional and sex differences in spontaneous striatal dopamine transmission. J Neurochem 160:598–612.

Castner SA, Xiao L, Becker JB (1993) Sex differences in striatal dopamine: in vivo microdialysis and behavioral studies. Brain Res 610:127–134.

Clark JJ, Sandberg SG, Wanat MJ, Gan JO, Horne EA, Hart AS, Akers CA, Parker JG, Willuhn I, Martinez V, Evans SB, Stella N, Phillips PEM (2010) Chronic microsensors for longitudinal, subsecond dopamine detection in behaving animals. Nat Methods 7:126–129.

Cummings JA, Jagannathan L, Jackson LR, Becker JB (2014) Sex differences in the effects of estradiol in the nucleus accumbens and striatum on the response to cocaine: neurochemistry and behavior. Drug Alcohol Depend 135:22–28.

DeWaele M, Oh Y, Park C, Kang YM, Shin H, Blaha CD, Bennet KE, Kim IY, Lee KH, Jang DP (2017) A baseline drift detrending technique for fast scan cyclic voltammetry. The Analyst 142:4317–4321.

Dluzen DE, McDermott JL (2008) Sex differences in dopamine- and vesicular monoamine-transporter functions. Ann N Y Acad Sci 1139:140–150.

Floresco SB (2015) The nucleus accumbens: an interface between cognition, emotion, and action. Annu Rev Psychol 66:25–52.

Garris PA, Christensen JR, Rebec GV, Wightman RM (1997) Real-time measurement of electrically evoked extracellular dopamine in the striatum of freely moving rats. J Neurochem 68:152–161.

Garris PA, Wightman RM (1995) Regional Differences in Dopamine Release, Uptake, and Diffusion Measured by Fast-Scan Cyclic Voltammetry. In: Voltammetric methods in brain systems, pp 179–220. New Jersey: Humana Press. Available at: http://link.springer.com/10.1385/0-89603-312-0:179 [Accessed June 19, 2023].

Hamid AA, Pettibone JR, Mabrouk OS, Hetrick VL, Schmidt R, Vander Weele CM, Kennedy RT, Aragona BJ, Berke JD (2016) Mesolimbic dopamine signals the value of work. Nat Neurosci 19:117–126.

Hu M, Becker JB (2003) Effects of sex and estrogen on behavioral sensitization to cocaine in rats. J Neurosci 23:693–699.

Huan Y, Gill JP, Fritzinger JB, Patel PR, Richie JM, Della Valle E, Weiland JD, Chestek CA, Chiel HJ (2021) Carbon fiber electrodes for intracellular recording and stimulation. J Neural Eng 18.

Karamihalev S, Brivio E, Flachskamm C, Stoffel R, Schmidt MV, Chen A (2020) Social dominance mediates behavioral adaptation to chronic stress in a sex-specific manner. eLife 9 Available at: http://dx.doi.org/10.7554/eLife.58723 [Accessed June 19, 2023].

Lee H, Jang M, Kim W, Noh J (2017) Differential effects of pair housing on voluntary nicotine consumption: a comparison between male and female adolescent rats. Psychopharmacology (Berl) 234:2463–2473.

Lynd-Balta E, Haber SN (1994) The organization of midbrain projections to the striatum in the primate: sensorimotor-related striatum versus ventral striatum. Neuroscience 59:625–640.

McWain MA, Pace RL, Nalan PA, Lester DB (2022) Age-dependent effects of social isolation on mesolimbic dopamine release. Exp Brain Res 240:2803–2815.

Moench KM, Logrip ML (2021) Housing Condition Differentially Impacts Escalation of Alcohol Intake, Relapse-Like Drinking, Anxiety-Like Behavior, and Stress History Effects by Sex. Alcohol Clin Exp Res 45:480–489.

Montague PR, McClure SM, Baldwin PR, Phillips PEM, Budygin EA, Stuber GD, Kilpatrick MR, Wightman RM (2004) Dynamic Gain Control of Dopamine Delivery in Freely Moving Animals. J Neurosci 24:1754–1759.

Nader MA, Nader SH, Czoty PW, Riddick NV, Gage HD, Gould RW, Blaylock BL, Kaplan JR, Garg PK, Davies HM, Morton D, Garg S, Reboussin BA (2012) SOCIAL DOMINANCE IN FEMALE MONKEYS: DOPAMINE RECEPTOR FUNCTION AND COCAINE REINFORCEMENT. Biol Psychiatry 72:414–421.

Novoa J, Rivero CJ, Pérez-Cardona EU, Freire-Arvelo JA, Zegers J, Yarur HE, Santiago-Marerro IG, Agosto-Rivera JL, González-Pérez JL, Gysling K, Segarra AC (2021) Social isolation of adolescent male rats increases anxiety and K+ -induced dopamine release in the nucleus accumbens: Role of CRF-R1. Eur J Neurosci 54:4888–4905.

Patel PR, Popov P, Caldwell CM, Welle EJ, Egert D, Pettibone JR, Roossien DH, Becker JB, Berke JD, Chestek CA, Cai D (2020) High density carbon fiber arrays for chronic electrophysiology, fast scan cyclic voltammetry, and correlative anatomy. J Neural Eng 17:056029.

Paulson PE, Robinson TE (1995) Amphetamine-induced time-dependent sensitization of dopamine neurotransmission in the dorsal and ventral striatum: a microdialysis study in behaving rats. Synap N Y N 19:56–65.

Puthongkham P, Lee ST, Venton BJ (2019) Mechanism of Histamine Oxidation and Electropolymerization at Carbon Electrodes. Anal Chem 91:8366–8373.

Quigley JA, Logsdon MK, Turner CA, Gonzalez IL, Leonardo NB, Becker JB (2021) Sex differences in vulnerability to addiction. Neuropharmacology 187:108491.

Rivest R, Falardeau P, Di Paolo T (1995) Brain dopamine transporter: gender differences and effect of chronic haloperidol. Brain Res 692:269–272.

Robinson TE, Becker JB (1982) Behavioral sensitization is accompanied by an enhancement in amphetamine-stimulated dopamine release from striatal tissue in vitro. Eur J Pharmacol 85:253–254.

Rossi LM, Reverte I, Ragozzino D, Badiani A, Venniro M, Caprioli D (2020) Role of nucleus accumbens core but not shell in incubation of methamphetamine craving after voluntary abstinence. Neuropsychopharmacology 45:256–265.

Samaha A-N, Khoo SY-S, Ferrario CR, Robinson TE (2021) Dopamine “ups and downs” in addiction revisited. Trends Neurosci 44:516–526.

Schindelin J, Arganda-Carreras I, Frise E, Kaynig V, Longair M, Pietzsch T, Preibisch S, Rueden C, Saalfeld S, Schmid B, Tinevez J-Y, White DJ, Hartenstein V, Eliceiri K, Tomancak P, Cardona A (2012) Fiji - an Open Source platform for biological image analysis. Nat Methods 9:10.1038/nmeth.2019.

Song Z, Yang H, Peckham EM, Becker JB (2019) Estradiol-Induced Potentiation of Dopamine Release in Dorsal Striatum Following Amphetamine Administration Requires Estradiol Receptors and mGlu5. eNeuro 6 Available at: http://eneuro.org/lookup/doi/10.1523/ENEURO.0446-18.2019 [Accessed June 19, 2023].

Takmakov P, McKinney CJ, Carelli RM, Wightman RM (2011) Instrumentation for fast-scan cyclic voltammetry combined with electrophysiology for behavioral experiments in freely moving animals. Rev Sci Instrum 82:074302.

Walker QD, Rooney MB, Wightman RM, Kuhn CM (2000) Dopamine release and uptake are greater in female than male rat striatum as measured by fast cyclic voltammetry. Neuroscience 95:1061–1070.

Welle EJ, Patel PR, Woods JE, Petrossians A, Della Valle E, Vega-Medina A, Richie JM, Cai D, Weiland JD, Chestek CA (2020) Ultra-small carbon fiber electrode recording site optimization and improved in vivo chronic recording yield. J Neural Eng 17:026037.

West EA, Carelli RM (2016) Nucleus Accumbens Core and Shell Differentially Encode Reward-Associated Cues after Reinforcer Devaluation. J Neurosci 36:1128–1139.

Westenbroek C, Perry AN, Becker JB (2013) Pair housing differentially affects motivation to self-administer cocaine in male and female rats. Behav Brain Res 252:68–71.

Westenbroek C, Perry AN, Jagannathan L, Becker JB (2019) Effect of social housing and oxytocin on the motivation to self-administer methamphetamine in female rats. Physiol Behav 203:10–17.

Westenbroek C, Ter Horst GJ, Roos MH, Kuipers SD, Trentani A, den Boer JA (2003) Gender-specific effects of social housing in rats after chronic mild stress exposure. Prog Neuropsychopharmacol Biol Psychiatry 27:21–30.

Willuhn I, Burgeno LM, Everitt BJ, Phillips PEM (2012) Hierarchical recruitment of phasic dopamine signaling in the striatum during the progression of cocaine use. Proc Natl Acad Sci U S A 109:20703–20708.

Wu Z, Lin D, Li Y (2022) Pushing the frontiers: tools for monitoring neurotransmitters and neuromodulators. Nat Rev Neurosci 23:257–274.

Xiao L, Becker JB (1994) Quantitative microdialysis determination of extracellular striatal dopamine concentration in male and female rats: effects of estrous cycle and gonadectomy. Neurosci Lett 180:155–158.